

# Modeling of the Hysteresis Phenomena in Finite-Sized Slitlike Nanopores. Revision of the Recent Results by Rigorous Numerical Analysis

Piotr Kowalczyk,<sup>\*,†,‡</sup> Katsumi Kaneko,<sup>†</sup> Lech Solarz,<sup>§</sup> Artur P. Terzyk,<sup>\*,||</sup>  
Hideki Tanaka,<sup>†</sup> and Robert Holyst<sup>‡</sup>

*Department of Chemistry, Faculty of Science, Chiba University, 1-3 Yayoi, Chiba 263, Japan; Department III, Institute of Physical Chemistry, Polish Academy of Science, Kasprzaka Street 44/52, 01-224 Warsaw, Poland; Military Technical Academy, Kaliski Street 2, 00-908 Warsaw, Poland; and Physicochemistry of Carbon Materials Research Group, Department of Chemistry, N. Copernicus University, Gagarin Street 7, 87-100 Torun, Poland*

Received January 14, 2005. In Final Form: April 16, 2005

The systematic investigation of the hysteresis phenomena in finite-sized slitlike nanopores via the Aranovich–Donohue (AD) lattice density functional theory (LDFT) is presented. The new reliable quantitative modeling of the adsorption and desorption branch of the hysteresis loop, through the formation and movement of the curved meniscus, is formulated. As a result, we find that our proposal, which closely mimics the experimental findings, can reproduce a rounded shape of the desorption branch of the hysteresis loop. On the basis of the exhausted commutations, we proved that the hysteresis loop obtained in the considered finite-sized slitlike geometry is of the H<sub>1</sub> type of the IUPAC classification. This fundamental result and the other most important results do not confirm the results of the recent studies of Sangwichien et al., whereas they fully agree with the recent lattice studies due to Monson et al. We recognize that the nature of the hysteresis loops (i.e. position, width, shape, and the multiple steps) mainly depends on the value of the energy of both the adsorbate–adsorbate and adsorbate–adsorbent interactions; however, the first one is critical for the appearance of hysteresis. Thus, for relatively small adsorbate–adsorbate interactions, the adsorption–desorption process is fully reversible in the whole region of the bulk density. We show that the strong adsorbate–adsorbent interactions produce (also observed experimentally) multiple steps within hysteresis loops. Contrary to the other studies of the hysteresis phenomena in confined geometry via the LDFT formalism, we constructed both ascending and descending scanning curves, which are known from the experimental observations. Additionally, we consider the problem of the stability of both the obtained adsorption and desorption branches of the computed hysteresis loop in finite-sized slitlike nanopores.

## 1. Introduction

Hysteresis phenomena have been observed on the adsorption–desorption isotherms for many systems. This is attributed to the nucleation difficulties,<sup>1</sup> reorientation effects,<sup>2</sup> the differences in the mechanisms of adsorption and desorption,<sup>3</sup> chemisorption,<sup>4,5</sup> the changes in the structure of an adsorbent and the sieving effect,<sup>6–10</sup> the differences in the vapor pressures of solid and liquid formed in the pores,<sup>11–15</sup> and the pore connectivity effect

and pore blocking.<sup>16–21</sup> An important paper concerning the last effect has been published by Sarkisov and Monson.<sup>22</sup> They concluded that the theories of hysteresis formulated on the concept of pore blocking (i.e. the traditional picture of adsorption and desorption in an ink-bottled pore) are not supported by the results of computer simulations. On the other hand, the mentioned authors confirmed the traditional mechanism of hysteresis and the Cohan model in simple cylindrical and slitlike pores. Recently, Mezzasalma<sup>23</sup> presented the general method which can be applied to any hysteresis phenomenon, and he concluded that the variational criterion of maximum entropy production can be successfully used for the description of adsorption–desorption data. This concept leads to different shapes of hysteresis loops.

Generally, neglecting chemisorption, the hysteresis on the adsorption–desorption isotherms in mesoporous

\* To whom correspondence should be addressed: P.K. e-mail, pkow@pchem2.s.chiba-u.ac.jp; A.P.T. e-mail, aterzyk@chem.uni.torun.pl.

† Chiba University.

‡ Polish Academy of Science.

§ Military Technical Academy.

|| N. Copernicus University.

(1) Bah, A.; Dupont-Pavlovsky, N.; Duval, X. *Surf. Sci.* **1996**, *352*, 518.

(2) Onishi, S.; Ohmori, T.; Ohkubo, T.; Noguchi, H.; Hanzawa, Y.; Kanoh, H.; Kaneko, K. *Appl. Surf. Sci.* **2002**, *196*, 81.

(3) Iiyama, T.; Ruike, N.; Kaneko, K. *Chem. Phys. Lett.* **2000**, *331*, 359.

(4) Tamon, H.; Okazaki, M. *J. Colloid Interface Sci.* **1996**, *179*, 181.

(5) Terzyk, A. P. *J. Colloid Interface Sci.* **2003**, *268*, 301.

(6) Patrykiewicz, A.; Sokołowski, S.; Sokołowska, Z.; Pizio, O. *J. Phys.: Condens. Matter* **2001**, *13*, 6151.

(7) Gales, L.; Mendes, A.; Costa, C. *Carbon* **2000**, *38*, 1083.

(8) Rychlicki, G.; Terzyk, A. P. *J. Therm. Anal.* **1995**, *45*, 1183.

(9) Rychlicki, G.; Terzyk, A. P.; Zawadzki, J. *Pol. J. Chem.* **1995**, *69*, 1328.

(10) Field, J. S.; Swain, M. V. *Carbon* **1996**, *34*, 1357.

(11) Morishige, K.; Kawano, K.; Hayashigi, T. *J. Phys. Chem. B* **2000**, *104*, 10298.

(12) Huber, P.; Knorr, K. *Phys. Rev. B.* **1999**, *60*, 12657.

(13) Molz, E. B.; Beamish, J. *J. Low Temp. Phys.* **1995**, *101*, 1055.

(14) Faivre, C.; Bellet, D.; Dolino, G. *Eur. Phys. J. B* **1999**, *7*, 19.

(15) Mackie, E. B.; Wolfson, R. A.; Arnold, L. M.; Lafdi, K.; Migone, A. D. *Langmuir* **1997**, *13*, 7197.

(16) Adkins, B. D.; Davis, B. H. *J. Phys. Chem.* **1986**, *90*, 4866.

(17) Morishige, K.; Nobuoka, K. *J. Chem. Phys.* **1997**, *107*, 6965.

(18) Lee, C. K.; Lee, S. L. *Heterog. Chem. Rev.* **1996**, *3*, 269.

(19) Liu, H.; Zhang, L.; Seaton, N. A. *J. Colloid Interface Sci.* **1993**, *156*, 285.

(20) Bhatia, S. K.; Liu, F.; Arvind, G. *Langmuir* **2000**, *16*, 4001.

(21) Maddox, M. W.; Lastoskie, C. M.; Quirke, N.; Gubbins, K. E. In *Fundamentals of Adsorption*; Le Van, M. D., Ed.; Boston, 1996; p 569.

(22) Sarkisov, L.; Monson, P. M. *Langmuir* **2001**, *17*, 7600.

(23) Mezzasalma, S. A. *J. Phys. Chem. B* **1999**, *103*, 7542.

materials is attributed to the occurrence of the capillary condensation process.<sup>24–31</sup> The classical methods based on the well-known Kelvin equation have been frequently used for the explanation of the hysteresis phenomenon. However, those basic concepts are limited to the macroscopic fluid characterized by the surface tension, bulk density, etc. As was pointed out by Kaneko et al.,<sup>32</sup> the classical capillary condensation theories, applying the above-mentioned Kelvin type relations, are a catastrophe for pores having widths smaller than ca. 4 nm (as determined from the nitrogen adsorption isotherm data measured at 77 K). Following Kaneko and co-workers,<sup>32</sup> we use the term “nanopores” for pores with diameters smaller than ca. 5 nm. What is the reason that such classical concepts of the capillary condensation are useless to the description of the hysteresis phenomena and/or the pore size distribution in nanopores? Nowadays, novel techniques of adsorption–desorption isotherm modeling such as grand canonical Monte Carlo (GCMC) simulations,<sup>33–43</sup> density functional theory (DFT),<sup>44–48</sup> molecular dynamics (MD),<sup>49</sup> nonequilibrium lattice fluids (NELFs),<sup>50</sup> and lattice density functional theory (LDFT) give a partial answer to this question. It is obvious that the concept of a macroscopic fluid in nanopores is very far from reality.<sup>51,52</sup> For a microscopic fluid placed in nanopores (i.e. in the external potential field generated by the pore walls), the concepts of surface tension and other macroscopic quantities are useless.<sup>29</sup> It was known from the results of

the above-mentioned advanced techniques of fluid modeling that the density of an adsorbed phase changes substantially with the distance from the pore surface.<sup>53</sup> This change has a periodical character, with the period being close to one collision diameter of a fluid atom. Moreover, it is commonly known from the results of the continuous DFT or molecular layer structure theory (MLST) that the external potential generated by a solid surface is a rapidly decreasing function.<sup>55–57</sup> Some empirical corrections of the standard methods based on the Kelvin relation have been proposed by many authors.<sup>58,59</sup> However, such corrections are purely empirical, and their utility is usually strongly limited to a selected kind of materials and to the specific pore geometry. Therefore, the above-mentioned classical methods overestimate the condensation pressure in nanopores.<sup>60</sup> A related nanopore size distribution function is shifted toward smaller values of pore widths for the slitlike geometry (or pore radius for the cylindrical one).<sup>61</sup> One of the most valuable theories of capillary condensation was developed by Derjaguin, Ulin, Broekhoff, and deBoer.<sup>62–64</sup> They improved the classical Kelvin concept of capillary condensation by taking into account the influence of the surface forces on the adsorbed film. We showed recently that this improvement (proposed almost 40 years ago) leads, for some mesoporous carbon fibers, to the same pore size distributions as those obtained from the application of the most advanced methods of mesoporosity calculation.<sup>65</sup> Consequently, this fundamental correction improved the relation between the filling pressure and the pore width; however, as was pointed by Ravikovitch et al., this concept also fails for small nanopores due to the macroscopic quantities used in calculations.<sup>60</sup>

The short description given above shows that the modeling of the hysteresis loops, which is the well-known difficult problem in the field of adsorption science, requires the novel concept of the description of the microscopic fluid placed in the nanopores. Among the techniques mentioned, the GCMC and the DFT techniques are the most powerful, but simultaneously, they are very time-consuming.<sup>66,67</sup> Moreover, as was pointed out by Ustinov and Do,<sup>57</sup> the classical NDFT approach cannot describe the adsorption on a simple carbon black surface without any empirical type relations (for example, introduction of empirical weight functions for correlation of the experimental data of nitrogen on Sterling FT carbon black). Thus, it is very hard to imagine how to use it for a both systematic

(24) Inoue, S.; Ichikuni, N.; Suzuki, T.; Uematsu, T.; Kaneko, K. *J. Phys. Chem. B* **1998**, *102*, 4689.

(25) Gusev, V. Y. *J. Colloid Interface Sci.* **1997**, *194*, 256.

(26) Inoue, S.; Hanzawa, Y.; Kaneko, K. *Langmuir* **1998**, *14*, 3079.

(27) Morishige, K.; Fujii, H.; Uga, M.; Kinukawa, D. *Langmuir* **1997**, *13*, 3494.

(28) Branton, P. J.; Sing, K. S. W.; White, J. W. *J. Chem. Soc., Faraday Trans.* **1997**, *93*, 2337.

(29) Llewellyn, P. L.; Grillet, Y.; Rouquerol, J.; Martin, C.; Coulomb J. P. *Surf. Sci.* **1996**, *352*, 468.

(30) Machin, W. D.; Murday, R. *J. Langmuir* **1996**, *12*, 6501.

(31) Inagaki, S.; Fukushima, Y.; Kuroda, K.; Kuroda, K. *J. Colloid Interface Sci.* **1996**, *180*, 623.

(32) Kaneko, K.; Ohba, T.; Hattori, Y.; Sunaga, M.; Tanaka, H.; Kanoh, H. In *Characterization of Porous Solids VI*; Rodriguez-Reinoso, F., McEnaney, B., Rouquerol, J., Unger, K., Eds.; Elsevier: Amsterdam, 2002; p 11.

(33) Papadopoulou, A.; Swol, F.; Marini, U.; Marconi, B. *J. Chem. Phys.* **1992**, *97*, 6942.

(34) Nicholson, D. *J. Chem. Soc., Faraday Trans.* **1994**, *90*, 181.

(35) Brodskaya, E. N.; Piotrovskaya, E. M. *Langmuir* **1997**, *13*, 6726.

(36) Maddox, M. W.; Gubbins, K. E. *Langmuir* **1995**, *11*, 3988.

(37) Acharyya, A. M.; Stauffer, D. *Eur. Phys. J. B* **1998**, *5*, 571.

(38) Sarkisov, L.; Monson, P. M. *Langmuir* **2000**, *16*, 9857.

(39) Lopez, R. H.; Vidales, A. M.; Zgrablich, G. *Langmuir* **2000**, *16*, 6999.

(40) Vishnyakov, A.; Neimark, A. V. *Langmuir* **2003**, *19*, 3240.

(41) Kikkinides, E. S.; Kainourgiakis, M. E.; Stubos, A. K. *Langmuir* **2003**, *19*, 3338.

(42) Rees, R. J.; Mainwaring, D. E.; Snook, I. K. *J. Mol. Liq.* **2003**, *103*, 423.

(43) Pellenq, R. J.-M.; Levitz, P. E. *Mol. Phys.* **2002**, *100*, 2059.

(44) Kozak, E.; Chmiel, G.; Patrykiewicz, A.; Sokolowski, S. *Phys. Lett. A* **1994**, *189*, 94.

(45) Neimark, A. V.; Ravikovitch, P. I.; Grun, M.; Schuth, F.; Unger, K. K. *J. Colloid Interface Sci.* **1998**, *207*, 159.

(46) Neimark, A. V.; Ravikovitch, P. I.; Vishnyakov, A. *Phys. Rev. E* **2000**, *62*, 1493.

(47) Chmiel, G.; Henderson, D.; Sokolowski, S. *Pol. J. Chem.* **1997**, *71*, 630.

(48) Kierlik, E.; Monson, P. A.; Rosinberg, M. L.; Tarjus, G. *J. Phys.: Condens. Matter* **2002**, *14*, 9295.

(49) Heffelfinger, G. S.; Swol, F.; Gubbins, K. E. *J. Chem. Phys.* **1988**, *89*, 5202.

(50) Doghieri, F.; Sarti, G. C. *Macromolecules* **1996**, *29*, 7885.

(51) Ravikovitch, P. I.; Haller, G. L.; Neimark, A. V. *Adv. Colloid Interface Sci.* **1988**, *76–77*, 203.

(52) Lastoskie, C.; Quirk, N.; Gubbins, K. E. In *Equilibria and Dynamics of Gas Adsorption on Heterogeneous Solid Surfaces*; Rudzinski, W., Steele, W. A., Zgrablich, G., Eds.; Elsevier: Amsterdam, 1997; Vol. 104, p 745.

(53) Evans, R. In *Fundamentals of Inhomogeneous Fluids*; Henderson, D., Ed.; Marcel Dekker: New York, 1992; Chapter 3.

(54) Hansen, J. P.; McDonald, I. R. *Theory of Simple Liquids*; Academic Press: London, 1990.

(55) Olivier, J. P. *J. Porous Mater.* **1995**, *2*, 9.

(56) Ustinov, E. A.; Do, D. D. *J. Colloid Interface Sci.* **2002**, *253*, 247.

(57) Ustinov, E. A.; Do, D. D. *Langmuir* **2003**, *19*, 8349.

(58) Kruk, M.; Jaroniec, M. In *Surfaces of Nanoparticles and Porous Materials*; Schwarz, J., Contescu, C., Eds.; Marcel Dekker: New York, 1998; Chapter 17, p 443.

(59) Jaroniec, M.; Kruk, M.; Choma J. In *Fundamentals of Adsorption 7*; Kaneko, K., Kanoh, H., Hanazawa, Y., Eds.; International Adsorption Society: Chiba, Japan, 2002; p 570.

(60) Ravikovitch, P. I.; Neimark, A. V. *Colloids Surf., A* **2001**, *187–188*, 11.

(61) Lastoskie, C.; Gubbins, K. E.; Quirk, N. *J. Phys. Chem.* **1993**, *97*, 4786.

(62) Derjaguin, B. V. *Acta Physicochim. USSR* **1940**, *12*, 181.

(63) Broekhoff, J. C. P.; de Boer, J. H. *J. Catal.* **1967**, *9*, 8.

(64) Dubinin, M. M.; Kataeva, L. I.; Ulin, V. I. *Bull. Acad. Sci. USSR Chem.* **1977**, *26*, 459.

(65) Kowalczyk, P.; Gun'ko, V. M.; Terzyk, A. P.; Gauden, P. A.; Rong, H.; Ryu, Z.; Do D. D. *Appl. Surf. Sci.* **2003**, *206*, 67.

(66) Ravikovitch, P. I.; Vishnyakov, A.; Neimark, A. V. *Phys. Rev. E* **2001**, *64*, 011602.

(67) Tanaka, H. *Molecular Confinement in Nanopores* (Thesis); Graduate School of Science and Technology: Chiba University, 2002.

and accurate study of the hysteresis phenomena. Moreover, Schoen et al.<sup>68</sup> pointed out that the hysteresis in the GCMC simulations can be observed due to a failure of the Metropolis algorithm. So, according to Schoen and co-workers, the observed hysteresis in the GCMC simulations can rather be treated as a handicap of the methodology. On the other hand, Sarkisov and Monson<sup>69</sup> argued that the mechanism of the hysteresis could be similar in experiments and in the GCMC simulations, provided that the model of the adsorbent microstructure used in the simulations is sufficiently realistic. The treatment of the structureless potential, such as, for example, 10–4–3 derived by Steele, for the slitlike pore geometry is still the topic of heated discussions.<sup>70,71</sup> In other words, this potential function cannot describe some obvious, and known from the experimental results, features of the adsorption systems such as, for example, the edge effect or heterogeneity. Summing up, the modeling of the above-mentioned properties of an adsorption system is not simple both theoretically and computationally. Here, it is worth noting that Neimark et al.<sup>72</sup> successfully applied the nonlocal version of the DFT proposed by Tarazona, the GCMC, and the gauge cell methods for the modeling of the hysteresis loops in cylindrical pores (usually small mesopores). Neimark and co-workers compared the computational results determined for MCM type materials with the experimental ones. Good agreement between modeling and experimental hysteresis loops was observed. Neimark's studies were based on the van der Waals metastability concept.<sup>46</sup> The metastability argument was based on the notion that adsorption isotherms show a van der Waals loop at conditions below the 2D critical point. A first-order phase transition point is selected according to the equality of the grand potential function in both the liquid and gas phases or from the Maxwell rule of equal areas. However, Kierlik and co-workers<sup>73,74</sup> concluded (applying the DFT method) that the classical van der Waals picture of metastability fails, due to the appearance of many metastable states. They also concluded that the true equilibrium capillary phase transition may occur when the perturbation induced by a solid is sufficiently small, that hysteresis does not necessarily imply the existence of this phase transition, that the disappearance of the hysteresis loop is not associated with capillary criticality, and that thermodynamic consistency is violated along the adsorption–desorption isotherms. Here, it is important to point out that the GCMC simulations and nonlocal DFT usually use the simplified model of pore geometry (i.e. structureless, infinitely long cylinder or slit) typically applied in the advanced techniques due to computational efficiency. The most advanced methods frequently applied to investigation of the hysteresis phenomenon are based on the so-called “single pore model”. The introduction of more complicated models leads to very interesting results. Rocken and Tarazona<sup>75</sup> introduced the chemical heterogeneity produced by a periodic wall

potential. They observed the new mechanism of capillary condensation, characterized by the splitting of the equilibrium “gas–liquid” transition. Also, more complicated modes have been applied recently,<sup>76</sup> and among them, the so-called “corrugated pore structure model” (CPST) was also developed and used to describe some experimental systems.<sup>77</sup> The CPST treats an adsorbent as a medium composed of a sequence of cylindrical pore segments of a constant length and distributed diameter. After some simplifications, the condensation–evaporation phenomena and gas adsorption can be described by the theoretical equations. Unfortunately, this model is formulated on the basis of the classical Kelvin equation, so the validity is limited only to mesopores.<sup>78,79</sup>

Another interesting and very important concept of the modeling of the hysteresis phenomenon has been proposed by Aranovich and Donohue.<sup>80,81</sup> The Aranovich and Donohue (AD) formalism is based on the statistical lattice gas approach introduced by Ono and Kondo.<sup>82</sup> Recently, Donohue and co-workers have shown that the AD lattice density theory with the appropriate boundary conditions can be used for the modeling of hysteresis loops in a finite slitlike pore.<sup>80,81</sup> Moreover, this phenomenon cannot be observed for the case of infinite slitlike pores. We want to point out that the AD formalism was successfully applied for the description of mono- and multilayer adsorption on flat surfaces and for the description of solid surface heterogeneity.<sup>83–86</sup> The AD approach is particularly important due to the possibility of the prediction of different (and observed experimentally) shapes of adsorption isotherms. As was pointed out by Aranovich and Donohue,<sup>83</sup> the IUPAC classification of the adsorption isotherms is applicable only to the condensable vapors, and this classification does not predict that adsorption can be a decreasing function of the equilibrium pressure. In fact, there are many experimental data measured under supercritical conditions, showing that the Gibbs excess can be a decreasing function of the pressure. It is worth pointing out that the AD theory (similarly to other lattice models) suffers from the severe limitations imposed by confining adsorbate molecules to the lattice sites. Moreover, similarly to the classical Ising lattice model, only the nearest-neighbor interactions are considered, the shape and polarity of an adsorbent is neglected, and so on. Particularly, the restriction of interactions to the nearest-neighbors omits the possibility of longer range cooperative effects which may be vital in smaller pores. From the above-mentioned limitations, we can suspect that the AD lattice approach can work well in dense, low temperature adsorbates but is useless for unconfined fluid states. Since the lattice formulation comes from the theory of solids, the solidlike adsorbate structure frequently

(68) Schoen, M.; Rhykerd Jr., C. L.; Cushman, J. H.; Diestler, D. J. *Mol. Phys.* **1989**, *66*, 1171.

(69) Sarkisov, L.; Monson, P. A. In *Fundamentals of Adsorption 7*; Kaneko, K.; Kanoh, H.; Hanazawa, Y., Eds.; International Adsorption Society: Chiba, Japan, 2002; p 327.

(70) Dobruskin, V. Kh. *Carbon* **2002**, *40*, 659.

(71) Do, D. D.; Do, H. D. *Adsorpt. Sci. Technol.* **2003**, *21*, 389.

(72) Neimark, V. A.; Ravikovitch, P. I.; Vishnyakov, A. In *Fundamentals of Adsorption 7*; Kaneko, K.; Kanoh, H.; Hanazawa, Y., Eds.; International Adsorption Society: Chiba, Japan, 2002; p 319.

(73) Kierlik, E.; Monson, P. A.; Rosinberg, M. L.; Sarkisov, L.; Tarjus, G. *Phys. Rev. Lett.* **2001**, *87*, 055710.

(74) Kierlik, E.; Rosinberg, M. L.; Tarjus, G.; Viot, P. *Phys. Chem. Chem. Phys.* **2001**, *3*, 1201.

(75) Rocken, S.; Tarazona, P. *J. Chem. Phys.* **1996**, *105*, 2034.

(76) Rojas, F.; Kornhauser, I.; Felipe, C.; Esparza, J. M.; Cordero, S.; Dominguez, A.; Riccardo J. R. *Phys. Chem. Chem. Phys.* **2002**, *4*, 2346.

(77) Salmas, C. E.; Ladavos, A. K.; Skaribas, S. P.; Pomonis, P. J.; Androutopoulos, G. P. *Langmuir* **2003**, *19*, 8777.

(78) Androutopoulos, G. P.; Salmas, C. S. *Ind. Eng. Chem. Res.* **2000**, *39*, 3747.

(79) Androutopoulos, G. P.; Salmas, C. S. *Ind. Eng. Chem. Res.* **2000**, *39*, 3764.

(80) Donohue, M. D.; Aranovich, G. L. *J. Colloid Interface Sci.* **1998**, *205*, 121.

(81) Sangwichien, C.; Aranovich, G. L.; Donohue, M. D. *Colloids Surf., A* **2002**, *206*, 313.

(82) Ono, S.; Kondo, S. In *Encyclopedia of Physics*; Flügge, S., Ed.; Springer: Berlin, 1960; Vol. 10, p 134.

(83) Aranovich, G. L.; Donohue, M. D. *J. Colloid Interface Sci.* **1998**, *200*, 273.

(84) Aranovich, G. L.; Donohue, M. D. *Phys. Rev. E* **1992**, *60*, 5552.

(85) Kowalczyk, P.; Tanaka, H.; Kanoh, H.; Kaneko, K. *Langmuir* **2004**, *20*, 2324.

(86) Kowalczyk, P.; Kaneko, K.; Terzyk, A. P.; Tanaka, H.; Kanoh, H.; Gauden, P. A. *Carbon* **2004**, *42*, 1813.

present in pores of molecular diameters can be described properly after reasonable rescaling of the energetic parameters on a lattice. Evidently, it seems clear that the studies on the AD approach, formulated on the grounds of the statistical thermodynamics, should be continued.

This manuscript is organized as follows. In the first part, we introduce the concept of so-called “kinetically controlled experiments”. Next, we describe the numerical problem and give the final numerical algorithm which can be used for the systematic investigation of hysteresis phenomena in finite-sized slitlike nanopores. For clarity, we present a detailed picture of the fluid evolution during the kinetically controlled experiments for a arbitrarily selected adsorbate–adsorbent system. At the end of the first part, we extend the concept of the kinetically controlled experiments by generating the ascending–descending scanning curves. In the next part, titled Insights into the Aranovich–Donohue Idea: Stability Investigations, we prove that the AD concept of the hysteresis phenomena modeling in the finite-sized slitlike pores is numerically stable. To do this, we incorporate the original methodology and simple algorithms. Finally, we present selected computational results and summarize the conclusions obtained from the kinetically controlled experiments. In all the cases, we try to relate the purely theoretical modeling to the examples found for experimental systems. We also show that the AD model can be used for modeling of the stable hysteresis loops in the finite-sized slitlike nanopores. Moreover, we show that the hysteresis loops are always characterized by a usually well developed perpendicular shape (i.e. H<sub>1</sub> type in the IUPAC classification). This phenomenon is physically justified, since such a type of the hysteresis loop, according to classical book of Gregg and Sing, is mainly attributed to the uniform material characterized by high homogeneity of pores. Moreover, the recent DFT and GCMC results confirm this thesis.

Our approach gives a better understanding of the hysteresis phenomenon in nanopores; however, further investigations will be the subject of forthcoming communications. Additional effects such as the heterogeneity of the walls, connectivity, and others will be the interest of our group in future reports.

## 2. Lattice DFT in the Finite-Sized Slitlike Pores and Kinetically Controlled Experiments

In this part, we briefly present the concept of the lattice DFT via the AD formalism for the finite-sized slitlike pores.

The main idea of Aranovich and Donohue used in the formulation of the hysteresis phenomena in the finite-sized slitlike pores comes straight from the fundamental Everett’s statement:<sup>87</sup> “We shall not discuss the unresolved problem of the applicability of the Kelvin equation to the case in which the radii approaches a few times the molecular diameter. It may be commented, however, that although there will no doubt, be quantitative deviations from this equations (and these deviations may be quite large), the fundamental kinetic factors that lead to this equation for the macroscopic systems will still manifest themselves in microscopic systems.”

Moreover, as we briefly mentioned above, Sarkisov and Monson,<sup>69</sup> applying the most advanced statistical mechanics simulation techniques (i.e. the molecular dynamics of adsorption and desorption by diffuse mass transfer and classical grand canonical Monte Carlo simulation), proved the fundamental thesis of Everett. The above-mentioned

authors concluded that for the case of simple slitlike and cylindrical geometry (both open and close ends) the traditional Everett’s concept is valid. They also pointed out that “This process was qualitatively predicted by Cohan.”

Recently, Aranovich and Donohue developed the Ono–Kondo equation for three dimensions.<sup>88</sup> It can be written as

$$\ln \left[ \frac{\rho_{i,j,k}(1-\rho_\infty)}{\rho_\infty(1-\rho_{i,j,k})} \right] + (\rho_{i+1,j,k} + \rho_{i-1,j,k} + \rho_{i,j+1,k} + \rho_{i,j-1,k} + \rho_{i,j,k+1} + \rho_{i,j,k-1} - 6\rho_\infty)\alpha = 0 \quad (1)$$

where  $\alpha = \epsilon/k_bT$ ,  $\epsilon$  is the adsorbate–adsorbate energy of interaction on the lattice,  $k_b$  is the Boltzmann constant, and  $T$  is the temperature. As usual, the minus interaction energy denotes the attractive forces and the positive one denotes the repulsion.

Equation 1 is the three-dimensional analogue of the classical one-dimensional Ono–Kondo equation. It relates the local density in each site  $(i,j,k)$  to the density in adjacent sites and in the bulk. Equation 1 is applicable to all sites with  $i^2 + j^2 + k^2 > 1$ . For site  $(1,0,0)$  the boundary condition is defined by

$$\ln \left[ \frac{\rho_{1,0,0}(1-\rho_\infty)}{\rho_\infty(1-\rho_{1,0,0})} \right] + (1 + \rho_{2,0,0} + \rho_{1,1,0} + \rho_{1,0,1} + \rho_{1,-1,0} + \rho_{1,0,-1} - 6\rho_\infty)\alpha = 0 \quad (2)$$

Sites  $(2,0,0)$ ,  $(1,1,0)$ ,  $(1,0,1)$ ,  $(1,-1,0)$ , and  $(1,0,-1)$  are the neighbors around site  $(1,0,0)$ . In eq 2 we assumed that there is a molecule at  $(0,0,0)$ . Other boundary conditions are  $\rho_{0,1,0} = \rho_{0,0,1} = \rho_{-1,0,0} = \rho_{0,-1,0} = \rho_{0,0,-1} = \rho_{1,0,0}$ . It seems obvious that eqs 1 and 2 can be applied, by the incorporation of different appropriate boundary conditions, for the description of mono- and multilayer adsorption on the flat surfaces and/or adsorption in finite-sized or infinite slitlike pores.<sup>88</sup> The boundary conditions are introduced through the nearest-neighbor attractions–repulsions in the layers adjacent to the pore walls.

For a slitlike finite length pore, the three-dimensional density distribution can be reduced to the two-dimensional one  $(\rho_{i,j})$ . As was shown by Aranovich and co-workers,<sup>88</sup> the minimization of the free energy leads to a system of nonlinear finite equations. However, we propose in this study to simplify the numerical problem by introducing symmetry into the finite-sized slitlike pore. This can be done in two ways (see Figure 1). For the case of even numbers of both adsorbent (equal to  $2N$ ) and adsorbate molecules (equal to  $2M$ ), the dividing planes are placed within  $N - (N + 1)$  and  $M - (M + 1)$ , respectively. On the other hand, for the case of odd numbers of both adsorbent (equal to  $2N + 1$ ) and adsorbate molecules (equal to  $2M + 1$ ), the dividing planes are running through the  $N$  and  $M$  molecule centers, respectively. This is the starting point of the novel method proposed in this study. For the case of even as well as odd numbers of both adsorbent and adsorbate molecules, our unknowns,  $\rho_{i,j}$ ,  $i \in \overline{1,M}$ , and  $j \in \overline{1,N}$ , are the solution of the following system of nonlinear finite equations:

$$\ln \left[ \frac{\rho_{i,j}(1-\rho_\infty)}{(1-\rho_{i,j})\rho_\infty} \right] = -h_{i,j}; \quad i \in \overline{1,M}; \quad j \in \overline{1,N} \quad (3)$$

where for odd numbers of adsorbate and adsorbent

(87) Everett, D. H., In *The Solid–Gas Interface*; Flood, E. A., Ed.; Marcel Dekker: New York, 1967.

molecules the right-hand side (RHS) matrix  $h_{i,j}$  is given by

$$h_{1,1} = \alpha(\beta + \rho_{i+1,j} + \rho_{i,j+1} + 2\rho_{i,j} - 5\rho_\infty), \quad i = 1, \quad j = 1 \quad (3.1a)$$

$$h_{1,j} = \alpha(\beta + \rho_{i+1,j} + \rho_{i,j-1} + \rho_{i,j+1} + 2\rho_{i,j} - 6\rho_\infty), \quad i = 1, \\ j = 2, 3, \dots, N - 1 \quad (3.2a)$$

$$h_{1,N} = \alpha(\beta + \rho_{i+1,j} + 2\rho_{i,j-1} + 2\rho_{i,j} - 6\rho_\infty), \quad i = 1, \\ j = N \quad (3.3a)$$

$$h_{i,1} = \alpha(\rho_{i-1,j} + \rho_{i+1,j} + \rho_{i,j+1} + 2\rho_{i,j} - 5\rho_\infty), \\ i = 2, 3, \dots, M - 1, \quad j = 1 \quad (3.4a)$$

$$h_{i,j} = \alpha(\rho_{i-1,j} + \rho_{i+1,j} + \rho_{i,j-1} + \rho_{i,j+1} + 2\rho_{i,j} - 6\rho_\infty), \\ i = 2, 3, \dots, M - 1, \quad j = 2, 3, \dots, N - 1 \quad (3.5a)$$

$$h_{i,N} = \alpha(\rho_{i-1,j} + \rho_{i+1,j} + 2\rho_{i,j-1} + 2\rho_{i,j} - 6\rho_\infty), \\ i = 2, 3, \dots, M - 1, \quad j = N \quad (3.6a)$$

$$h_{M,1} = \alpha(2\rho_{i-1,j} + \rho_{i,j+1} + 2\rho_{i,j} - 5\rho_\infty), \quad i = M, \quad j = 1 \\ (3.7a)$$

$$h_{M,j} = \alpha(2\rho_{i-1,j} + \rho_{i,j-1} + \rho_{i,j+1} + 2\rho_{i,j} - 6\rho_\infty), \quad i = M, \\ j = 2, 3, \dots, N - 1 \quad (3.8a)$$

$$h_{M,N} = \alpha(2\rho_{i-1,j} + 2\rho_{i,j-1} + 2\rho_{i,j} - 6\rho_\infty), \quad i = M, \\ j = N \quad (3.9a)$$

For the second case, i.e., even numbers of both adsorbent and adsorbate molecules, the RHS matrix  $h_{i,j}$  is defined as follows:

$$h_{1,1} = \alpha(\beta + \rho_{i+1,j} + \rho_{i,j+1} + 2\rho_{i,j} - 5\rho_\infty), \quad i = 1, \quad j = 1 \\ (3.1b)$$

$$h_{1,j} = \alpha(\beta + \rho_{i+1,j} + \rho_{i,j-1} + \rho_{i,j+1} + 2\rho_{i,j} - 6\rho_\infty), \quad i = 1, \\ j = 2, 3, \dots, N - 1 \quad (3.2b)$$

$$h_{1,N} = \alpha(\beta + \rho_{i+1,j} + \rho_{i,j-1} + 3\rho_{i,j} - 6\rho_\infty), \quad i = 1, \\ j = N \quad (3.3b)$$

$$h_{i,1} = \alpha(\rho_{i-1,j} + \rho_{i+1,j} + \rho_{i,j+1} + 2\rho_{i,j} - 5\rho_\infty), \\ i = 2, 3, \dots, M - 1, \quad j = 1 \quad (3.4b)$$

$$h_{i,j} = \alpha(\rho_{i-1,j} + \rho_{i+1,j} + \rho_{i,j-1} + \rho_{i,j+1} + 2\rho_{i,j} - 6\rho_\infty), \\ i = 2, 3, \dots, M - 1, \quad j = 2, 3, \dots, N - 1 \quad (3.5b)$$

$$h_{i,N} = \alpha(\rho_{i-1,j} + \rho_{i+1,j} + \rho_{i,j-1} + 3\rho_{i,j} - 6\rho_\infty), \\ i = 2, 3, \dots, M - 1, \quad j = N \quad (3.6b)$$

$$h_{M,1} = \alpha(\rho_{i-1,j} + \rho_{i,j+1} + 3\rho_{i,j} - 5\rho_\infty), \quad i = M, \quad j = 1 \\ (3.7b)$$

$$h_{M,j} = \alpha(\rho_{i-1,j} + \rho_{i,j-1} + \rho_{i,j+1} + 3\rho_{i,j} - 6\rho_\infty), \quad i = M, \\ j = 2, 3, \dots, N - 1 \quad (3.8b)$$

$$h_{M,N} = \alpha(\rho_{i-1,j} + \rho_{i,j-1} + 4\rho_{i,j} - 6\rho_\infty), \quad i = M, \quad j = N \\ (3.9b)$$

where  $\beta = \epsilon_s/\epsilon$  and  $\epsilon_s$  denotes the energy of the interactions between an adsorbate and the surface atom.

The solution of eq 3, with the coefficients given by eqs 3.1–3.9, can be successfully obtained by the well-known successive approximation algorithm.<sup>89,90</sup> The efficiently

(88) Aranovich, G. L.; Donohue, M. D. *J. Chem. Phys.* **2000**, *112*, 2361.

(89) Lane, J. E. *Aust. J. Chem.* **1968**, *21*, 827.

(90) Korn, G. A.; Korn, T. M. *Mathematical Handbook for Scientists and Engineers*; McGraw-Hill: New York, 1961; Chapter 11.3.

obtained final results of the successive substitutions type algorithm are closely related to the initial guess for  $\rho_{i,j}$ :  $i \in \overline{1,M}; j \in \overline{1,N}$ . Moreover, we want to point out that the control of the error in the successive substitutions algorithm, especially in the hysteresis region characterized by the dual solution, is critical for the extrapolation to the unique stable solution (i.e. a branch of the hysteresis loop).

In the so-called kinetically controlled experiments introduced by Aranovich and Donohue,<sup>83</sup> the adsorption process can be modeled by the initial concave plane, and the desorption one is modeled by the initial convex plane. Clearly, these assumptions come from the Everett thesis. As we will show later, the differences between initial guesses for  $\rho_{i,j}$  can lead to the hysteresis loops.

In the developed successive substitution algorithm, we model the adsorption process by the following initial concave plane, given mathematically by (see Figure 2)

$$\rho_{i,j} = \rho_\infty \left[ (1 - \alpha) \cos\left(\frac{\pi}{2} \frac{ij}{MN}\right) + \alpha \right], \quad i \in \overline{1,M}; \quad j \in \overline{1,N} \quad (4)$$

On the other hand, the desorption process is modeled by the following initial convex plane expressed by (see Figure 2)

$$\rho_{i,j} = \rho_\infty + (b - \rho_\infty) \sin\left(\frac{\pi}{2} \frac{ij}{MN}\right), \quad i \in \overline{1,M}; \quad j \in \overline{1,N} \quad (5)$$

Here, both  $\alpha = 0.2$  and  $b = 0.92$  were chosen arbitrarily.

It should be noticed that from the physical point of view the initial functions given above seem to be a very reliable approximation of the real ones. They are precisely imitating the macroscopic two-dimensional menisci, since they are continuous and smooth as well.

For both the adsorption and desorption processes, the distance between the consecutive iterations (i.e.  $k - 1$  and  $k$ ) is defined by the following scalar quantity:

$$\Omega = \frac{1}{\rho_\infty} \sqrt{\frac{1}{MN} \sum_{i=1}^M \sum_{j=1}^N (\rho_{i,j}^{k-1} - \rho_{i,j}^k)^2} \quad (6)$$

Since the positions of the dividing planes (originating from the assumed symmetry) are different for the odd and even numbers of both adsorbate and adsorbent molecules (see Figure 1), the definition of the (measured experimentally) Gibbs adsorption excess is slightly different for both cases. Thus, for the even number of adsorbate and adsorbent molecules, we can define the excess Gibbs adsorption by

$$\Gamma = \frac{4}{MN} \sum_{i=1}^M \sum_{j=1}^N (\rho_{i,j} - \rho_\infty) \quad (7)$$

On the other hand, for the odd number of adsorbate and adsorbent molecules, we should define the excess Gibbs adsorption more precisely (see Figure 1):

$$\Gamma = \frac{1}{MN} \left( 4 \sum_{i=1}^{M-1} \sum_{j=1}^{N-1} (\rho_{i,j} - \rho_\infty) + 2 \sum_{i=1}^{M-1} (\rho_{i,N} - \rho_\infty) + \right. \\ \left. 2 \sum_{j=1}^{N-1} (\rho_{M,j} - \rho_\infty) + (\rho_{M,N} - \rho_\infty) \right) \quad (8)$$

On the basis of the above-introduced equations, the hysteresis phenomenon can be easily modeled by the kinetically controlled experiments.<sup>83</sup> As we mentioned

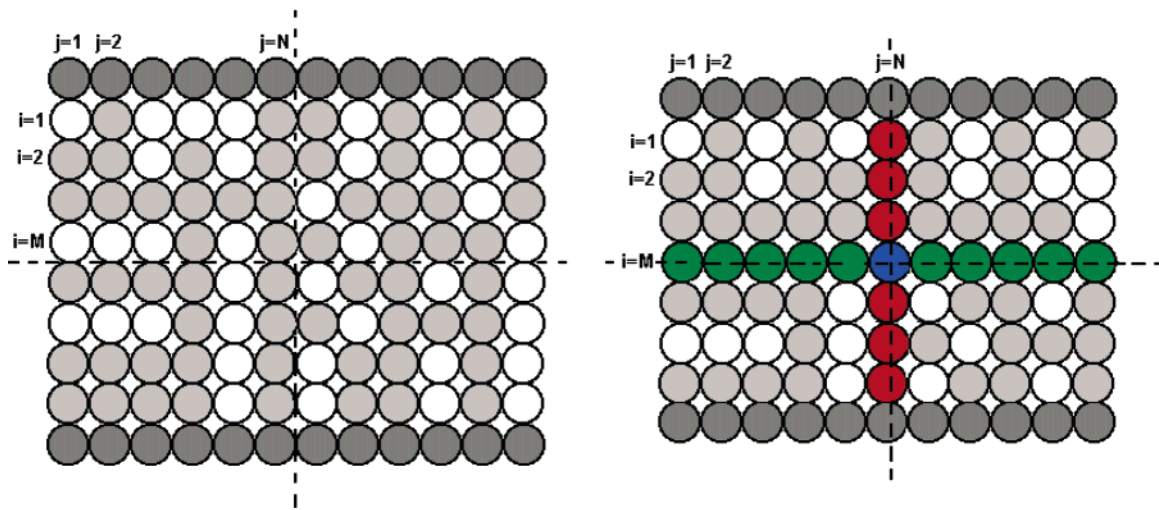


**Figure 1.** Model of the finite-sized slitlike pores. The left panel presents a pore consisting of even numbers of both adsorbate and adsorbent molecules (pore length  $2N$  and pore width  $2M$ ). The right panel presents a pore consisting of odd numbers of both adsorbate and adsorbent molecules (pore length  $2N - 1$  and pore width  $2M - 1$ ). Dashed lines are the symmetry axes.

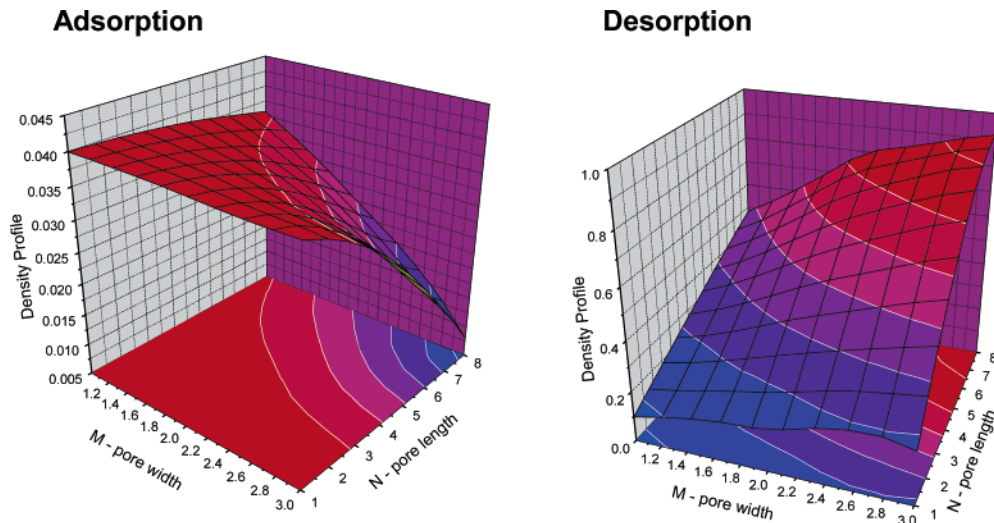


**Figure 2.** Initial two-dimensional density profile generated from eqs 4 (left panel) and 5 (right panel). The computations were performed for the following parameters:  $N = 15$ ,  $M = 5$ ,  $\alpha = -1.1$ , and  $\epsilon_s/k_bT = -1.2$ . The displayed profiles correspond to bulk density  $\rho_\infty = 0.04$ .

above, in this study we develop the numerical algorithm based on the classical successive substitution scheme. This type of numerical algorithm efficiently copes with the considered problem.

In Figures 3–5 we present the detailed microscopic description of the kinetically controlled experiments via the AD proposal for the arbitrary selected system.<sup>83</sup> As one can see, contrary to the infinitely long slitlike pores, the AD LDF model allows the formation and the disappearance of curved menisci at the open ends of the pores (see contour local density profiles displayed in Figures 4 and 5). For adsorption, the calculations start from the initial density profile given by eq 4 and adsorption is calculated as the density increases. As one can see from Figure 4, during the adsorption process, we observe a continuous thickening of the films on each wall until they reach the instability point (i.e. classical layer-by-layer condensation). For desorption, the calculations start with the initial density profile generated from eq 5 and desorption occurs as the density decreases. During desorption, the curved meniscus is formed and progressively recedes toward the center of the finite-sized slitlike pore, until it changes shape. Notice that for desorption the layer-by-layer evaporation occurs from the ends of the pore.

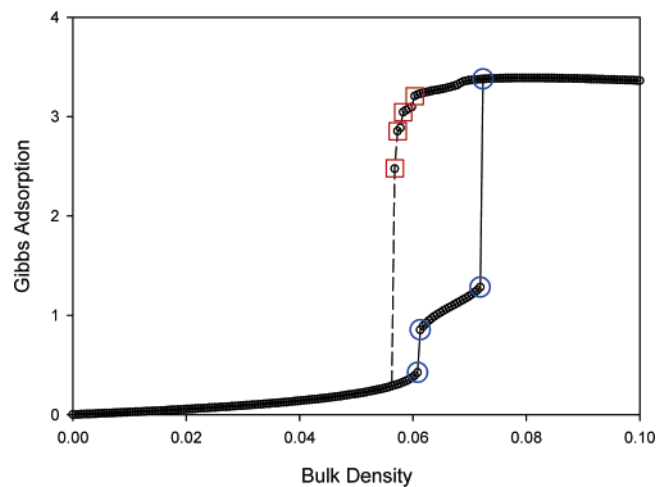


**Figure 3.** Gibbs excess adsorption isotherm for  $N = 30$ ,  $M = 6$ ,  $\alpha = -1.0$ , and  $\epsilon_s/k_bT = -1.0$ .

Such a mechanism of desorption is mapped to the rounded shape of the Gibbs surface excess isotherm; however, the rounded shape of the desorption branch is very sensitive

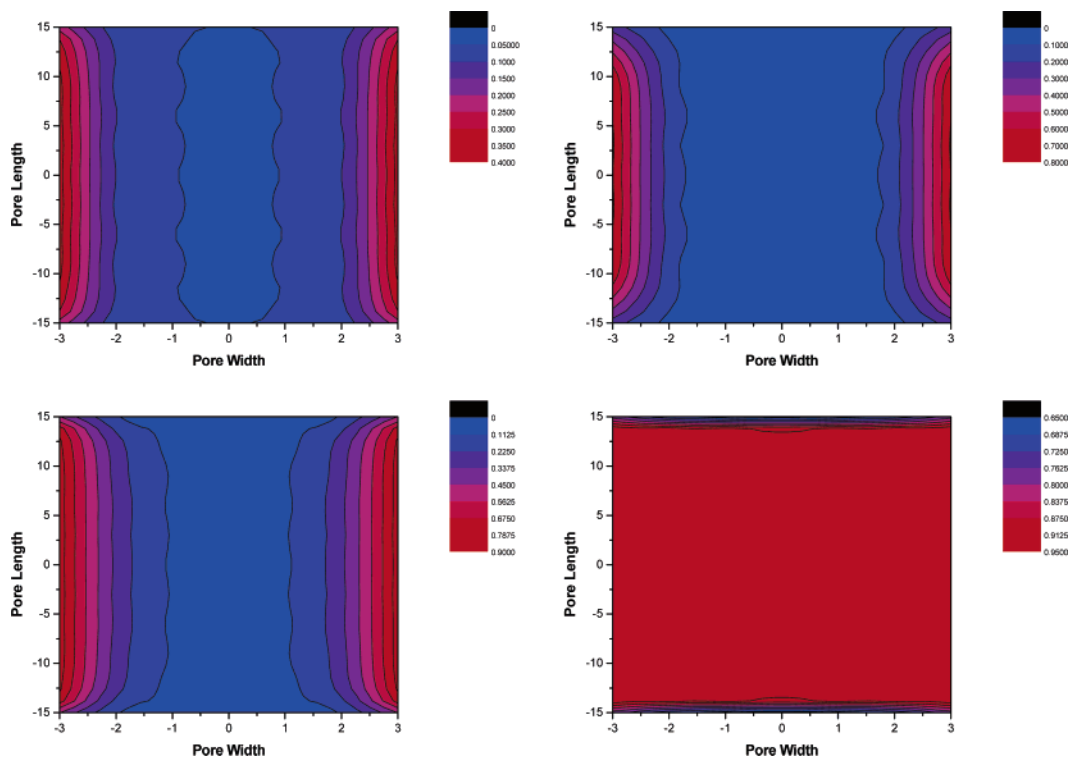


**Figure 4.** Adsorption in a finite-sized slitlike pore for  $N = 30$ ,  $M = 6$ ,  $\alpha = -1.0$ , and  $\epsilon_s/k_bT = -1.0$ . The final local density profiles correspond to the blue circles marked in Figure 3.

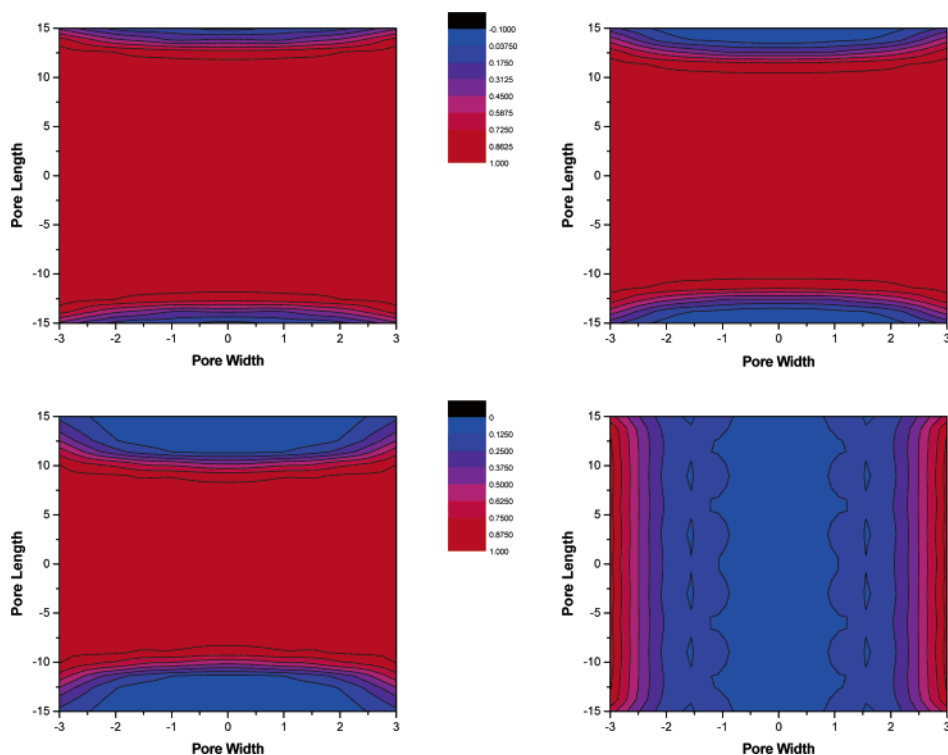


**Figure 5.** Desorption in a finite-sized slitlike pore for  $N = 30$ ,  $M = 6$ ,  $\alpha = -1.0$ , and  $\epsilon_s/k_bT = -1.0$ . The final local density profiles correspond to the red squares marked in Figure 3.

to the both adsorbate–adsorbate and adsorbate–adsorbent interaction parameters (see Figure 3).

According to Everett, the hysteresis loop displayed in Figure 3 is called the boundary loop or main loop. A further important feature of the experimental hysteresis loops is the presence of ascending and descending scanning curves within the range bounded by the main hysteresis loop. The ascending and descending scanning curves are observed experimentally when the adsorption–desorption

process is reversed at the selected point placed in the region of the main hysteresis loop.<sup>91</sup> Due to the change of the process direction, the system can return to the main hysteresis loop by different paths spanning between the adsorption and desorption branches of the main hysteresis loop. Obviously, the existence and characteristics of the

(91) Rouquerol, F.; Rouquerol, J.; Sing, K. S. W. *Adsorption by Powders and Porous Solids*; Academic Press: San Diego, 1999.

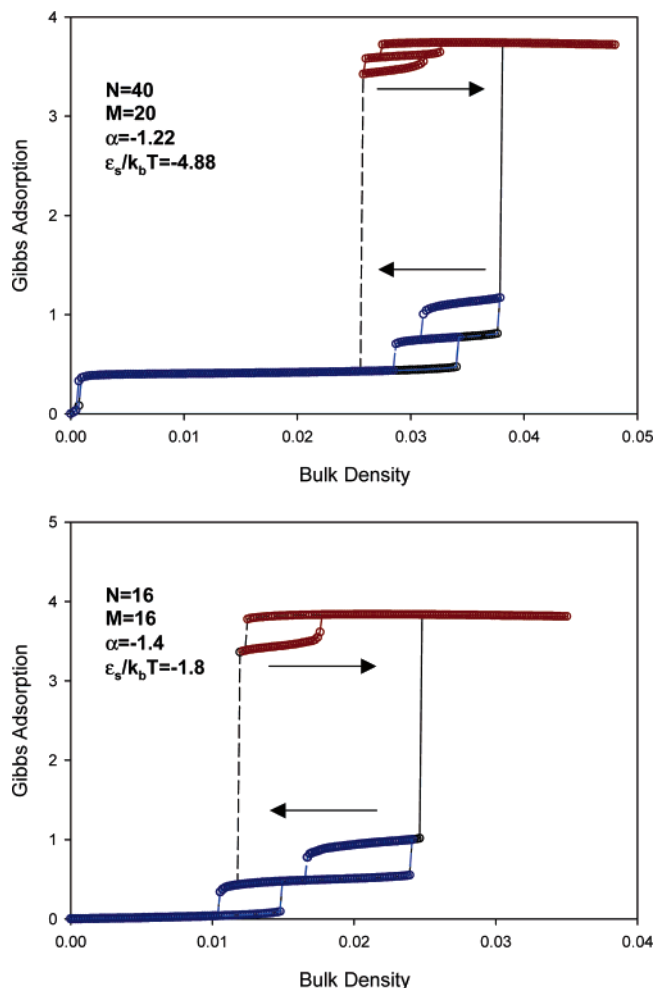


**Figure 6.** Illustration of the descending (blue lines) and ascending (red lines) scanning curves obtained from kinetically controlled experiments via the extended AD LDFT. The values of the parameters are displayed in the figure.

scanning behavior of an adsorbate–adsorbent system showing hysteresis are important factors which must be taken into account during development of the theory of the phenomenon. In the current paper, we extended the concept of the kinetically controlled experiments via the AD proposal to generate the ascending–descending scanning curves. This can be simply done by reversing the adsorption or desorption path during computations. In Figure 6 we prove that the extended AD kinetically controlled experiments via the LDFT method can generate the scanning curves; however, their nature is not investigated in this study. One thing is certain: that the scanning behavior in pure finite-sized slitlike pores is related to the presence of steps on the adsorption–desorption branch of the main hysteresis loop. The stepwise character of condensation–evaporation in finite-sized slitlike nanopores can only be observed for some adsorbate–adsorbent systems, usually characterized by relatively strong both adsorbate–adsorbate and adsorbate–adsorbent interactions. Consequently, not all adsorbate–adsorbent systems can generate ascending–descending scanning curves. Moreover, the ascending–descending scanning curves are bounded by the main hysteresis loop, as was suspected from the experimental results.

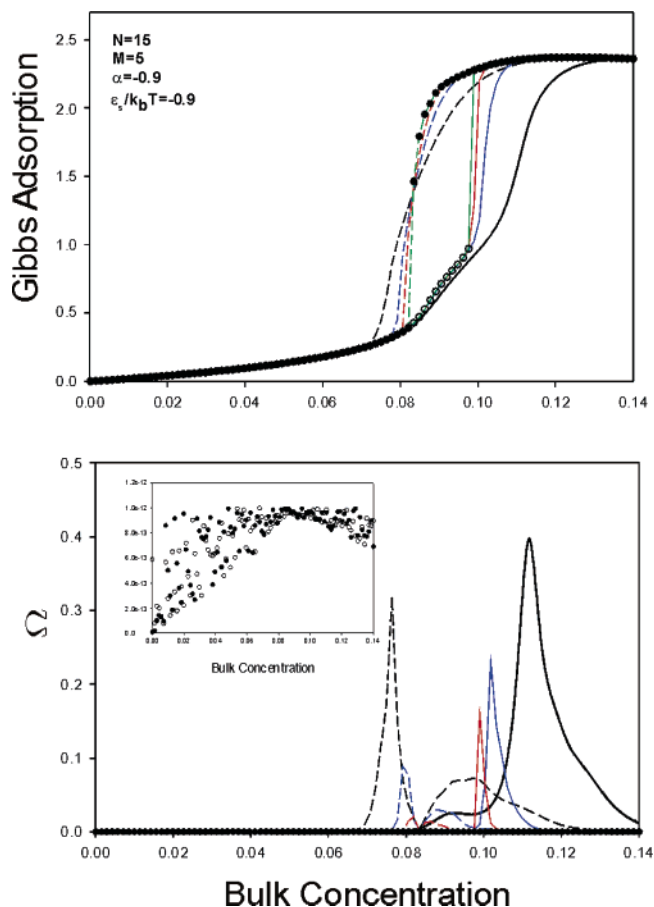


**Figure 7.** Rigorous numerical analysis of the hysteresis loop (adsorption branch, solid line/open circles; desorption one, short dashed line/closed circles) generated on the basis of the AD LDFT in the finite-sized slitlike nanopore (parameters are displayed in the picture). The calculations were performed for the following numbers of successive substitutions: black line, 30; blue line, 60; red line, 100; dark green line, 500; circles, 10000.

### 3. Insights into the Aranovich–Donohue Idea: Stability Investigations

The stability problem of the hysteresis phenomena is usually omitted by many authors because it is difficult to answer questions such as the following: *Do we evaluate the stable branches of the hysteresis loop? Did we detect all solutions of nonlinear equations? Are the solutions physically justified?* Moreover, in the investigations of the adsorption–desorption hysteresis phenomena, the classical Lapunov's<sup>92,93</sup> concepts of the “local” or “global” stability cannot be applied directly, since we do not know the dependence of the phenomena on time.

In the current paper, we introduce the concept of the “numerical stability”. At equilibrium, the grand potentials (i.e. minimized function) of all phases in the system are equal. This condition defines the equations of equilibrium derived by Aranovich et al. and presented above (i.e. eq 3 with the coefficients given by eqs 3.1–3.9). It is commonly known that the appearance of the hysteresis means exactly the possibility of the existence of multiple solutions of the nonlinear system of the equations given above. Clearly, not only the first-order phase transition can give the multiple solutions. As in our model, closely related to the AD proposal, the multiple solutions (here, exactly the branches of the hysteresis loop) can originate from different boundary conditions.

On the basis of the above-described classical concept of the hysteresis phenomena, we can suspect that adsorption

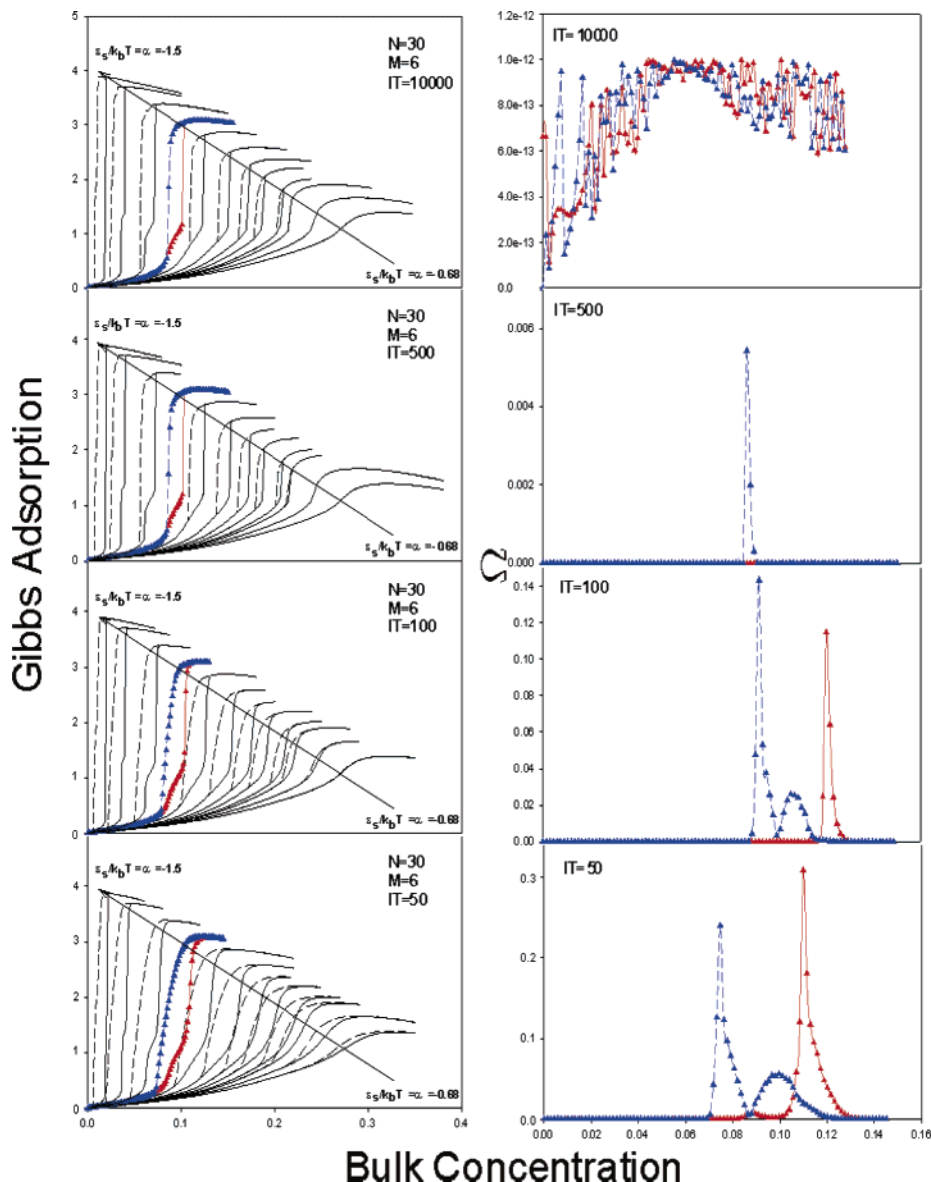


**Figure 8.** Influence of the insufficient number of the successive substitutions on the shape of the hysteresis loops for selected parameters given in the pictures (see left panel). The right panel shows the error plots for the arbitrary selected loops from the left panel.

can cause condensation at certain spots (like corners, edges, or just in the middle of the finite-sized slitlike pore—whatever). This picture of the condensation process is fully physically justified. On the other hand, the desorption process should be modeled by an initial convex plane, according to the well-known Cohan<sup>94</sup> proposal.

Here, another question appears: *What situation will occur when the initial density profiles represent the intermediate state between functions introduced for modeling both adsorption and desorption processes (i.e. eqs 4 and 5)?* In other words: *Is the final solution, generated from the initial intermediate density profile, the exact one among the branches of the hysteresis loop detected (applying the initial conditions given by eqs 4 and 5)?* If all initial intermediate density profiles always lead to the adsorption–desorption hysteresis loop generated on the basis of the initial conditions given by eq 4 or 5, then we can state that the modeling is numerically stable and, moreover, the obtained results are unique. Here, the term “all” should be treated as physically justified by the classical Cohan approach.<sup>94</sup>

To investigate the numerical stability of the hysteresis phenomena modeling according to the AD proposal, we

introduce the following additional initial density distribution functions, given by

$$\rho_{i,j} = \rho_{\infty} \left[ \left(1 - a\right) \left(\frac{ij}{MN}\right) + a \right] + \Pi(0, \zeta), \quad i \in \overline{1, M};$$

$$j \in \overline{1, N} \quad (9)$$

$$\rho_{i,j} = \rho_{\infty} \left[ a \cos\left(2\pi \frac{ij}{MN}\right) + 1 - a \right] + \Pi(0, \zeta), \quad i \in \overline{1, M};$$

$$j \in \overline{1, N} \quad (10)$$

$$\rho_{i,j} = \rho_{\infty} + (b - \rho_{\infty}) \sin\left(\frac{\pi}{2} \frac{ij}{MN}\right) + \Pi(0, \zeta), \quad i \in \overline{1, M};$$

$$j \in \overline{1, N} \quad (11)$$

Here,  $a = 0.2$  and  $b = 0.92$ . The Gaussian noise,  $\Pi(0, \zeta)$ , imitates some of the density fluctuations added to the initial density profile. Clearly, for the initial density profile, the conditions  $\rho_{i,j} \in [0, 1]$ ,  $i \in \overline{1, M}$ , and  $j \in \overline{1, N}$  should be fulfilled by the additional constraints.

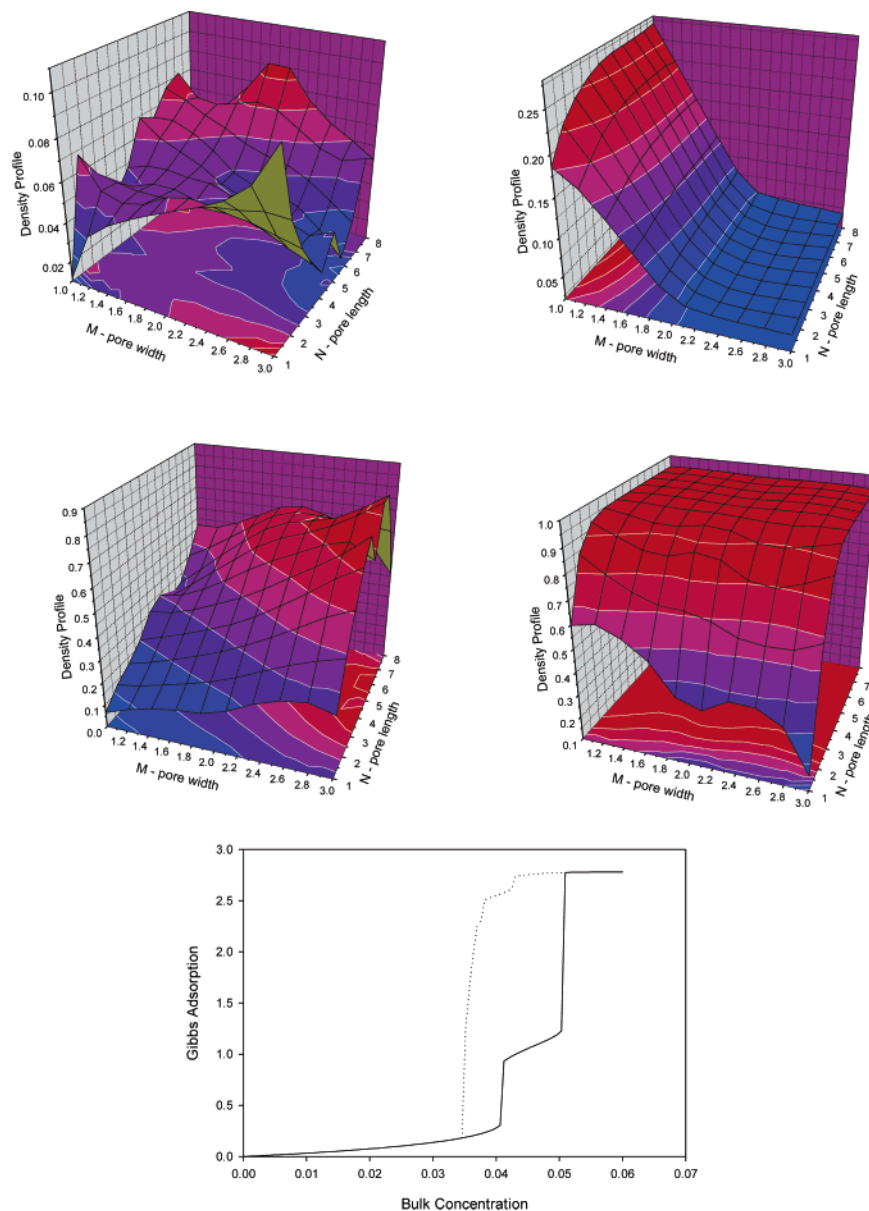


**Figure 9.** (Left panel) Initial two-dimensional density profile generated from eqs 10 and 11. (Right panel) Final density profile. The Gibbs excess adsorption–desorption isotherm is also presented at the bottom. The computations were performed for the following parameters:  $N = 15$ ,  $M = 5$ ,  $\alpha = -1.1$ ,  $\epsilon_s/k_bT = -1.2$ , and bulk density  $\rho_\infty = 0.04$ .

Summing up, our idea is to prove that, for a realistic model of the function modeling the initial two-dimensional density profile in the finite-sized slitlike nanopore and being the intermediate function given by eqs 4 and 5, the final results should always be the adsorption or desorption branch of the hysteresis loop.

#### 4. Results and Discussion

We performed a systematic study of the hysteresis phenomena in finite-sized slitlike nanopores. First of all, we paid more attention to the accuracy of the obtained solutions, since the shape of the hysteresis loop is closely related to them. In the above-cited paper of Sangwichien et al., the authors concluded that: “*It is shown that LDFT can predict adsorption isotherms with hysteresis loops and that different types of hysteresis loops can be obtained*

*by varying energies of adsorbate–adsorbate and adsorbate–adsorbent interactions for different widths and lengths of a slitlike pore.*” The authors introduced the classical successive substitution algorithm using Wolfram’s MATHEMATICA software.<sup>95</sup> However, they did not explain the details of the performed computations. We developed the original program based on the classical successive substitution scheme, exactly the same as that mentioned by Sangwichien et al.<sup>81</sup> Additionally, we monitored the errors between all successive iterations for all computed points. The selected final results, presented in Figures 7 and 8, are critical for the application and understanding of the hysteresis phenomena in the finite-sized slitlike nanopores via the AD LDFT formalism. Let us first pay attention to Figure 7, as we can suspect the problem of the accuracy of the computations is characteristic of the hysteresis region. For an insufficient number of successive substitutions (i.e. the small final accuracy), the loop is wide and is almost of the  $H_2$  type in the IUPAC

(92) Lapunov, A. M. *General Problem of Motion Stability*; ONTI: Moskov, 1935 (in Russian).

(93) Bogusz, W.; Dzygadło, Z.; Rogula, D.; Sobczyk, K.; Solarz, L. *Stud. Appl. Mech.* **1991**, *30*, 87.

(94) Cohan, L. H. *J. Am. Chem. Soc.* **1938**, *60*, 433.

(95) Wolfram, S. *The Mathematica Book*, 3rd ed.; Wolfram Media/Cambridge University Press: Cambridge, 1993.

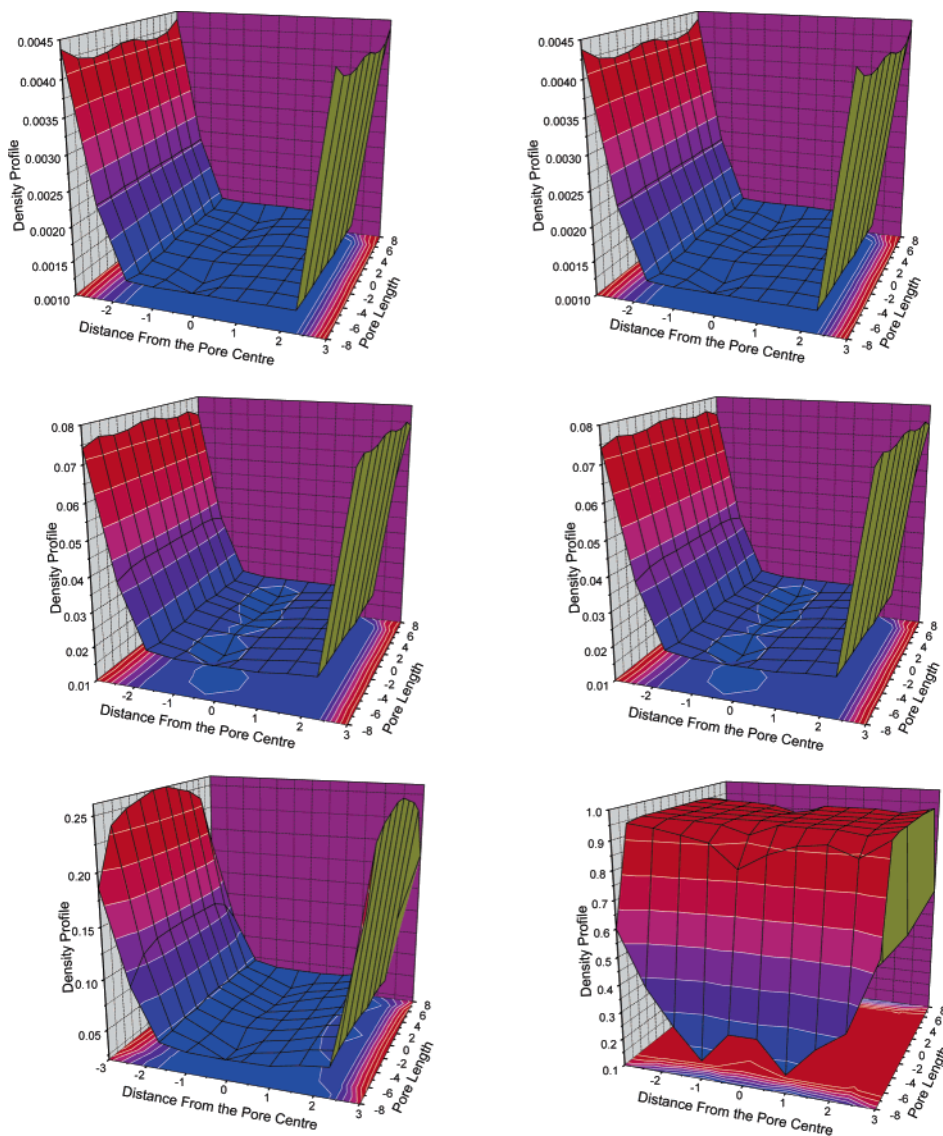


**Figure 10.** Final density profiles in the finite-sized slitlike pore ( $N = 15$ ,  $M = 5$ ,  $\alpha = -1.1$ ,  $\epsilon_s/k_bT = -1.2$ ) obtained for the selected density values in the bulk phase  $\rho_\infty = 0.0013$ ;  $0.02$ ;  $0.04$ . The left panels present the final adsorption density profiles, and the right ones display the final desorption ones.

classification.<sup>91</sup> However, for an increasing number of successive substitutions, the loops transform to the classical  $H_1$  type (i.e. the adsorption and desorption branches are almost vertical and nearly parallel to one another). Such a transformation is characterized by a gradual changing, and the final true hysteresis loop is narrower than that calculated with insufficient accuracy. From Figures 7 and 8 we can conclude that this is the general tendency. Thus, the following primary question arises: *What is the sufficient number of successive substitutions (i.e. the accuracy of the computations)?* To answer this question, we introduce the mathematical definition of the boundary. It means that the number of successive substitutions should be large enough that the final results cannot be dependent on them. In all our calculations, we assume the number of successive substitutions is equal to 10 000 (i.e. for all points, with and beyond the hysteresis region, the final accuracy is about  $1 \text{ e}^{-12}$ ). Clearly, as one can see from Figures 7 and 8, the hysteresis loops generated by the AD LDFT in the finite-sized slitlike nanopores are always of the type  $H_1$  (sometimes with additional steps due to the layering process) if the required accuracy is achieved.

Knowing the proper value of the control parameters of the considered model, we investigated the numerical stability introduced in the previous section. Some selected results from the large number of the performed numerical computations are presented in Figure 9 and in Supporting Information Figures 1S, 2S, and 3S. One can find the typical initial and corresponding final density profiles for the arbitrarily selected bulk density ( $\rho_\infty = 0.04$ ) from the hysteresis region. The corresponding Gibbs excess adsorption–desorption isotherm is also displayed. It can be concluded that the AD proposal is numerically stable and the final hysteresis loop is unique. This fact is worthy to be pointed out.

The scenario of the hysteresis phenomena obtained from the LDFT modeled by the kinetically controlled experiment is always very similar. As an example, in Figure 10 we present the dynamic creation of the hysteresis loop for the arbitrarily selected values of the parameters. Figure 10 presents the final density profiles for the adsorption (left panel) and desorption (right panel) branches of the hysteresis loop obtained from the LDFT for the arbitrarily selected density in the bulk phase. Beyond the hysteresis region, the final density profile in the finite-sized slitlike

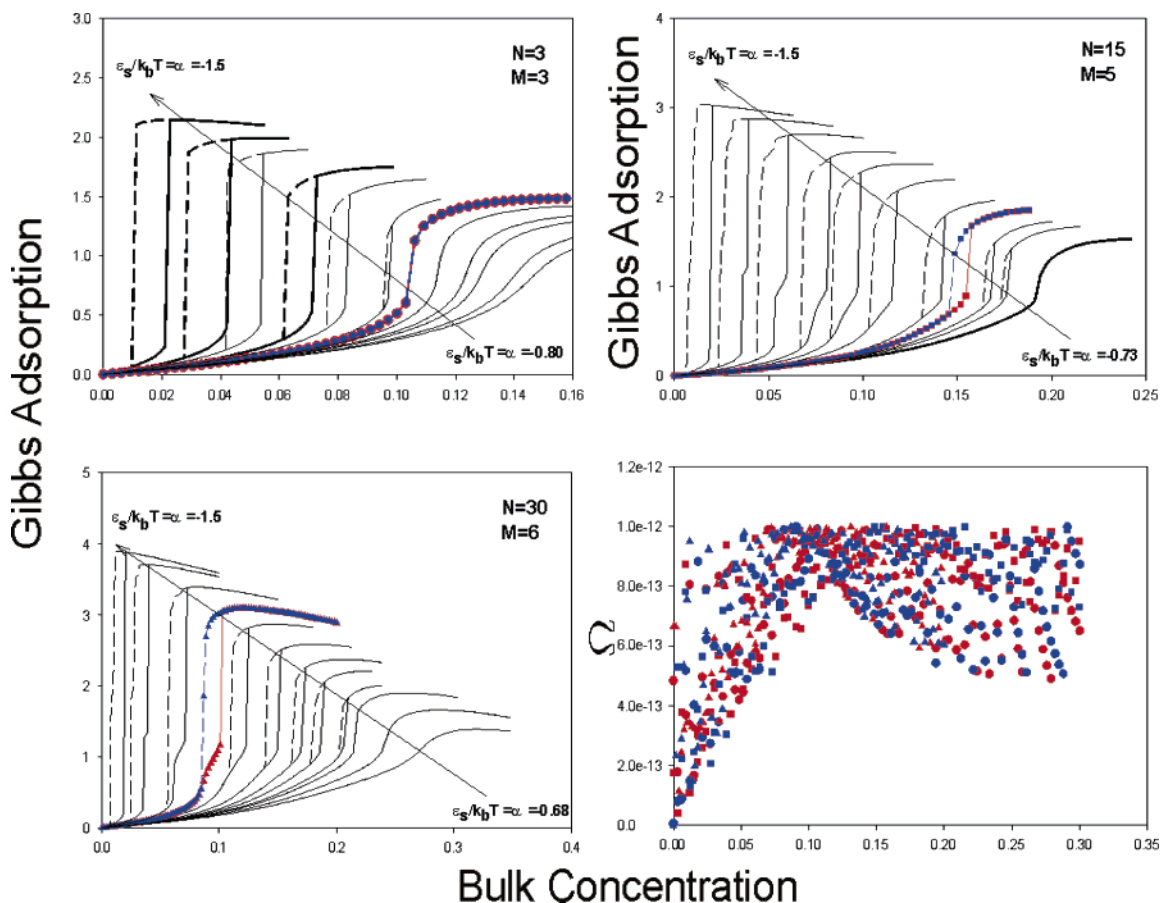


**Figure 11.** Excess adsorption–desorption isotherms in the finite-sized slitlike nanopores obtained from the Aranovich–Donohue LDFT. The values of the parameters are displayed in the figure. Solid line, adsorption branch; dashed line, desorption branch. The error of the successive substitution algorithm is displayed for the arbitrary selected hysteresis loops (for the last group of isotherms,  $N = 30$ ,  $M = 6$ ).

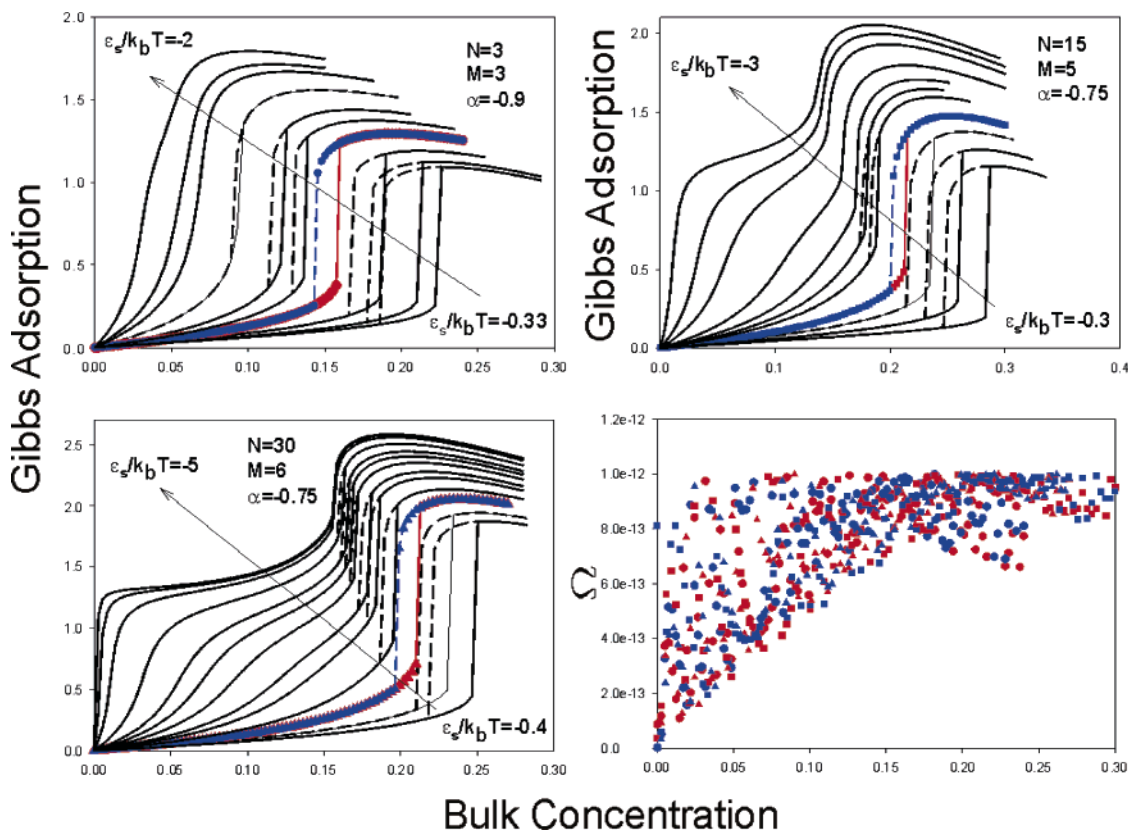


**Figure 12.** Data calculated for another set of parameters; the description is the same as that for Figure 11.

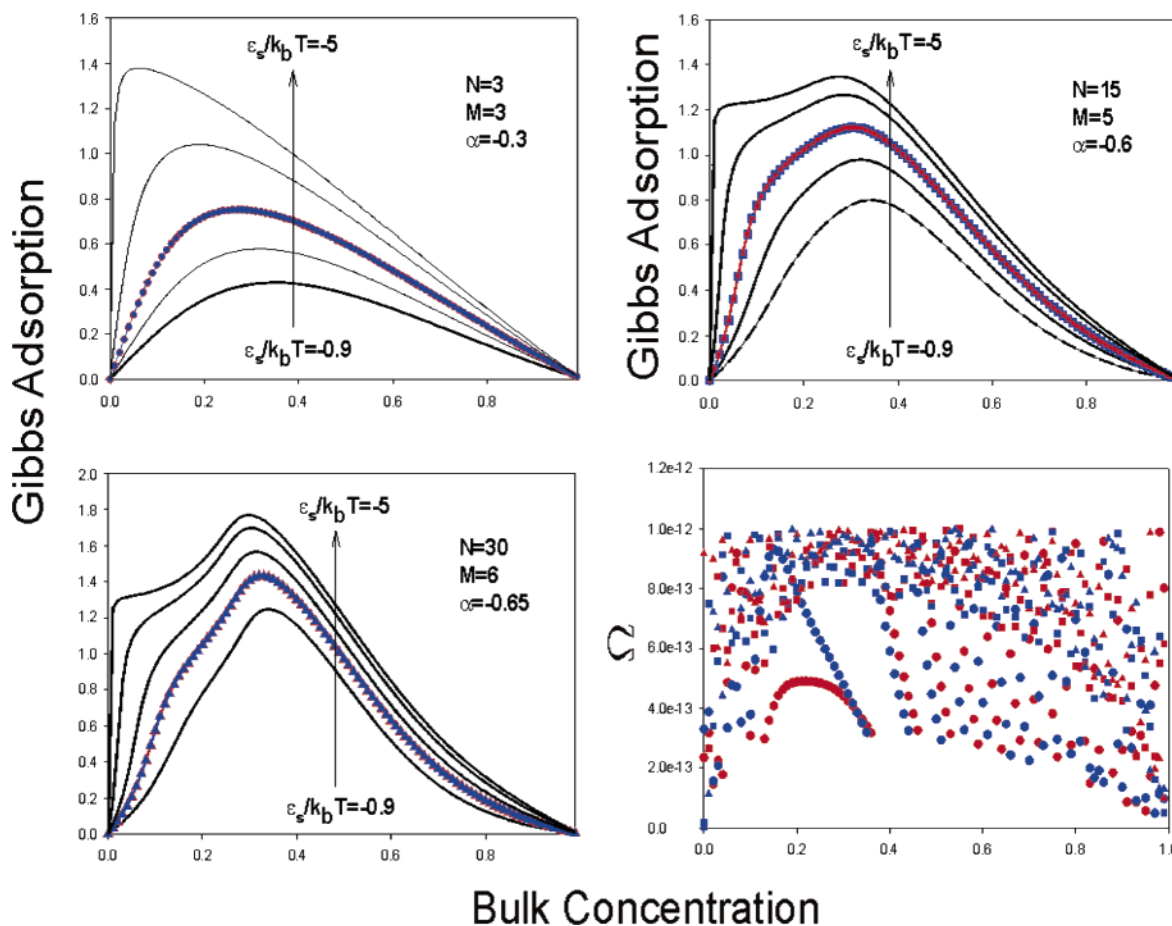


**Figure 13.** Data calculated for another set of parameters; the description is the same as that for Figure 11.

nanopore is the same for both the adsorption and desorption processes. In other words, adsorption is reversible and as a result the initial conditions (i.e. the initial density profile) do not influence the final results. However, for some values of the density in the bulk phase, the hysteresis is very lightly pronounced (see the bottom of Figure 10). Since the final two-dimensional density profile in the finite-sized slitlike nanopore is different for the adsorption and desorption processes, the resulting adsorption and desorption curves (i.e. the Gibbs excess of adsorption–desorption) diverge and hysteresis appears.

It is important that all our investigations do not refer to the concrete adsorption–desorption system, since they are done with dimensionless quantities. Consequently, our results, selectively displayed in Figures 11–14, can be regarded as general ones.

First, we explain the results presented in Figure 11. As one can see, the hysteresis loop can appear only when the energetic parameters are sufficiently large (i.e.  $\alpha = \epsilon_s/k_b T \cong -0.9 \div -0.7$ ). Moreover, the adsorption and desorption branches are always almost vertical and nearly parallel to one another. On the other hand, the size of the hysteresis loops changes regularly. For the relatively small values of both the adsorbate–adsorbate and adsorbent–adsorbate interactions, the hysteresis loop is narrow. The rise in the energy of the above-mentioned interactions leads to the widening of the hysteresis loop. It is worthy to emphasize that some additional steps on the adsorption and desorption hysteresis branches can appear. This phenomenon, also found in the continuous DFT method, comes from the competition between the layering and

condensation–evaporation processes.<sup>96,97</sup> From Figure 11 we can also conclude that, generally, the dimensions in the nanopore range slightly influence the hysteresis behavior. All generated hysteresis loops are characterized by the well-defined rounded desorption branches.

From Figure 12 one can conclude that hysteresis is well defined when the values of the adsorbate–adsorbate and adsorbate–adsorbent interaction energies are comparable. Clearly, the value of the energetic parameters should be large enough. Additionally, the results displayed in Figure 12 show that, for relatively weak adsorbate–adsorbate interactions and relatively strong adsorbate–adsorbent interaction energy, the hysteresis loops can disappear. Here, we also obtained a well-defined rounded desorption branch of all the computed hysteresis loops.

In Figure 13 we present the results of the computations for the very small adsorbate–adsorbate interaction energy and for the progressively increasing adsorbate–adsorbent one. The results are very interesting and confirm the following thesis: hysteresis loops never appear in the finite-sized slitlike nanopores if the adsorbate–adsorbate interaction is relatively small, contrary to the very high value of the adsorbate–adsorbent interactions. This fact is well-known from the experimental studies. As an example, the adsorption of nitrogen or hydrogen at supercritical conditions is always a reversible process. Under supercritical conditions, the thermal motion and relatively weak fluid–fluid interaction of molecules prevent the condensation and the densification of fluid in

(96) Stepniak, K.; Patrykiewicz, A.; Sokolowska, Z.; Sokolowski, S. *J. Colloid Interface Sci.* **1999**, *214*, 91.

(97) Franke, O.; Schulz-Ekloff, G.; Rathousky, J.; Starek, J.; Zukal, A. *J. Chem. Soc., Chem. Commun.* **1993**, *9*, 724.

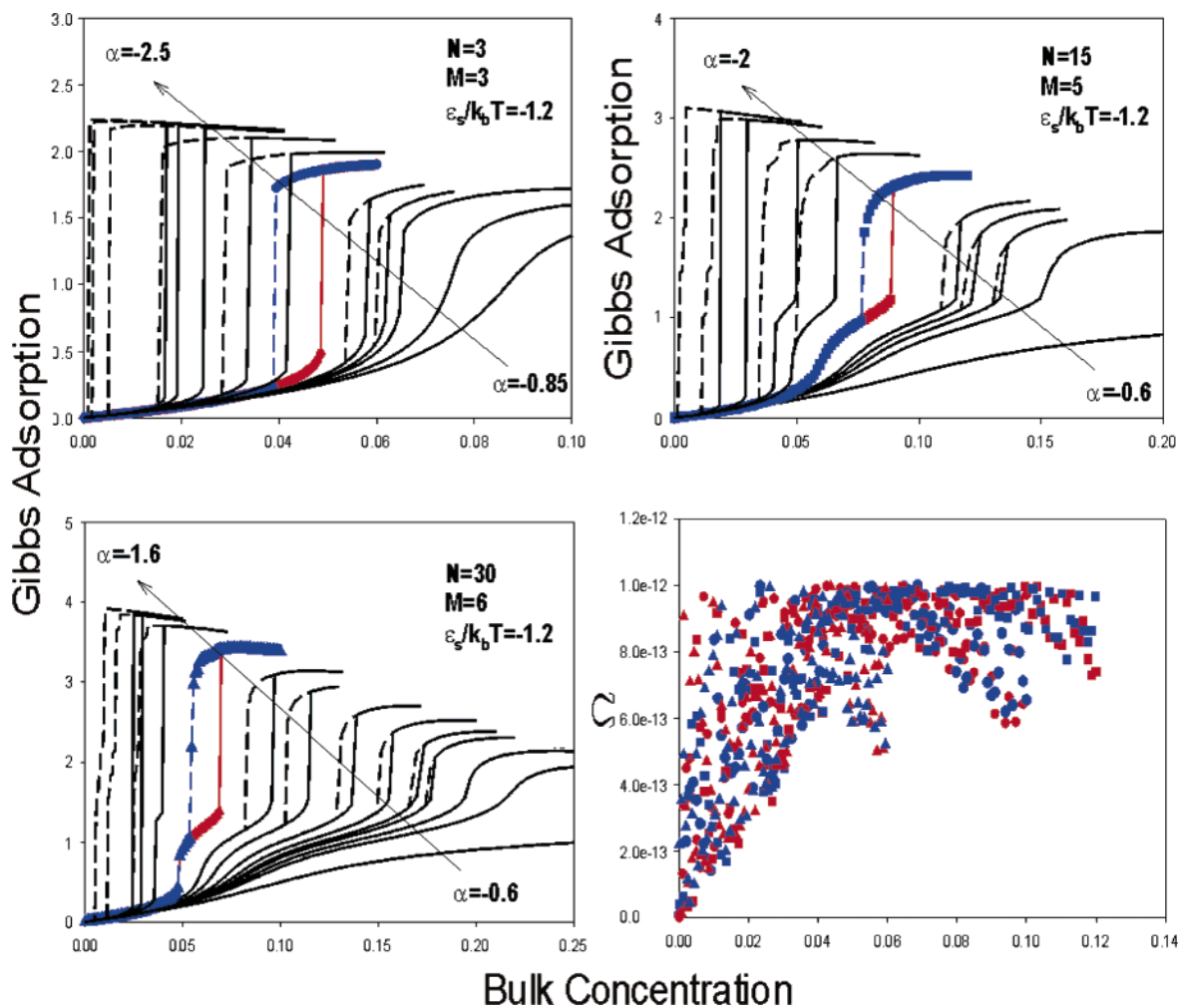


**Figure 14.** Data calculated for another set of parameters; the description is the same as that for Figure 11.

nanopores, resulting in a reversible adsorption–desorption isotherm.

Figure 14 displays the results of the hysteresis modeling, assuming relatively large adsorbate–adsorbent interactions (i.e.  $\epsilon_s/k_b T = -1.2$ ) and a progressive increase in the energy of adsorbate–adsorbate interactions. Here, the general trend in the hysteresis loop transformation is very similar to the one displayed in Figure 11. However, as one can observe, the steps on both the adsorption and desorption branches of the hysteresis loops are very lightly pronounced. This seems obvious, since the adsorbate–adsorbent interactions are assumed to be relatively high. It is worthy to emphasize that these are the experimental data exhibiting steps within the hysteresis loops.<sup>97</sup>

Summing up our computational results, we can state that the hysteresis in the finite-sized slitlike nanopores is mainly dependent on both the adsorbate–adsorbate and adsorbate–adsorbent interactions; however, the first ones seem to be critical for the appearance of the hysteresis loops. Generally, the increase in both types of interactions causes the progressive widening of the hysteresis loop. This statement can be regarded as a general one only if some critical values of the adsorbate–adsorbate interactions are exceeded. The problem of hysteresis disappearance can be assigned to the relatively weak adsorbate–adsorbent interactions and relatively high adsorbate–adsorbent ones. Finally, for the very weak adsorbate–adsorbate interactions, hysteresis is not expected.

Figure 15 shows the effect of temperature on the hysteresis shape and on the value of the Gibbs excess of

adsorption–desorption. We assume the equality of the adsorbate–adsorbate and adsorbate–adsorbent interaction energies. Next, we are progressively increasing the temperature (i.e. we reduce the interaction energies) for an arbitrarily chosen size of the slitlike nanopores. Consequently, the adsorption–desorption phenomenon is transformed from subcritical to supercritical conditions. As a result, the hysteresis loop is progressively decreased during simulated heating. In adsorption–desorption processes placed in supercritical conditions, the hysteresis effect practically disappears. The hysteresis loops presented in Figure 15 belong to the classical  $H_1$  type in the IUPAC classification. There are no changes of the hysteresis type during the simulated heating. The hysteresis is only lowering the loop during this modeling. Moreover, the rounded shape of the desorption branch for all generated hysteresis loops during the simulated heating is prevented.

The above-reported features were predicted by the DFT modeling<sup>98</sup> of adsorption–desorption phenomena and were also observed experimentally.<sup>97,99–109</sup>

(98) Evans, R. In *Microscopic Theories of Simple Fluids and Their Interfaces*; Charvolin, J., Joanny, J. F., Zinn-Justin, J., Eds.; Elsevier Science Publishers: Amsterdam, 1990; p 4.

(99) Bryk, P.; Reszko-Zygmunt, J.; Sokolowski, S. *Mol. Phys.* **1999**, *96*, 1509.

(100) Sing, K. S. W.; Everett, D. H.; Haul, R. A. W.; Moscou, L.; Pierotti, R. A.; Rouquerol, J.; Siemieniowska, T. *Pure Appl. Chem.* **1985**, *57*, 403.

(101) Thommes, M.; Kohn, R.; Froba, M. *J. Phys. Chem. B* **2000**, *104*, 7932.

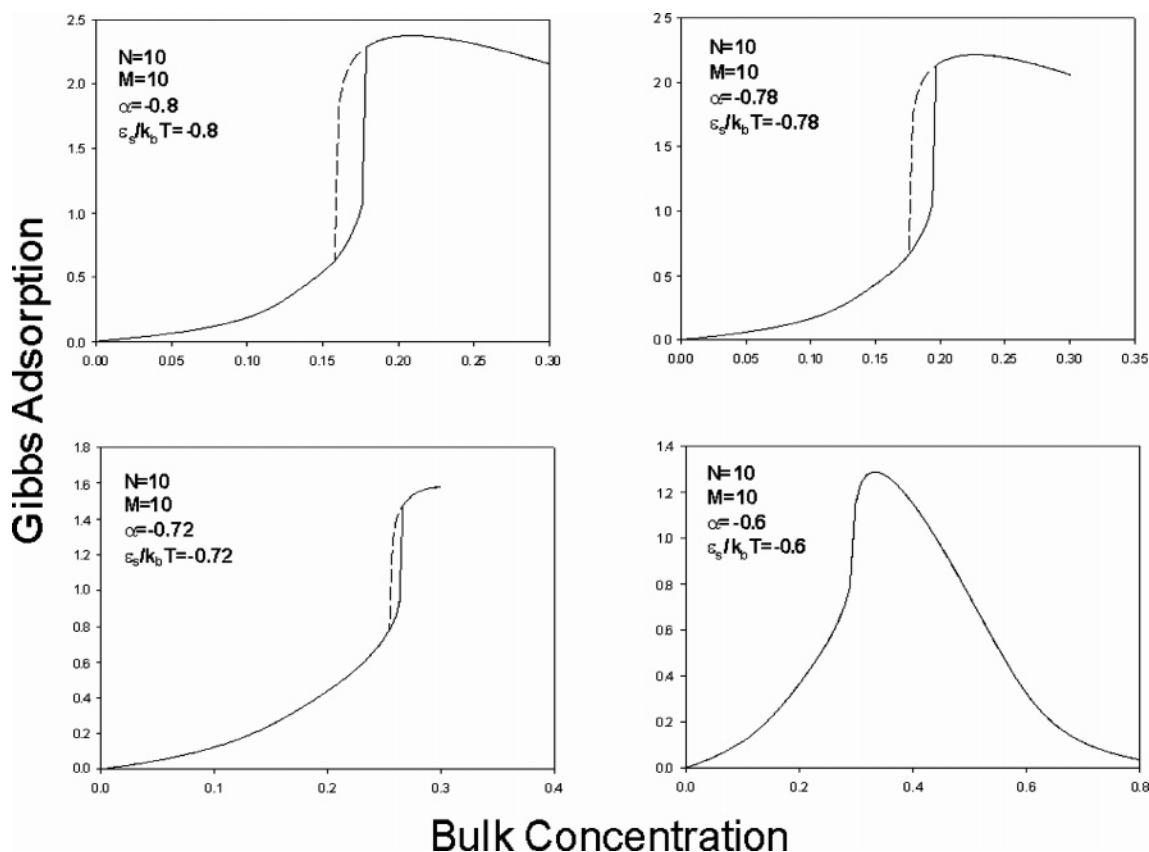


**Figure 15.** Effect of the temperature on the adsorption (solid lines)–desorption (dashed lines) isotherms.

## 5. Conclusions

The presented studies should be treated as basic ones. We do not precisely analyze the adsorption–desorption system; however, we prove (applying the idea of the kinetically controlled experiments) that hysteresis loops can be observed in finite-sized slitlike nanopores. According to the AD LDFT model, the hysteresis loop is a consequence of different boundary conditions (i.e. shape of the curved meniscus) which are modeled in the current work in a rigorous mathematical fashion. We find that the hysteresis phenomena in the considered geometry can be modeled by a microscopic model resulting in formation and movement of a curved meniscus. Such a mechanism is mapped into the rounded shape of the desorption branch of the hysteresis loop. In contrast to a recent paper of Sangwichien et al., we explain the real behavior of the hysteresis phenomena described on the basis of the AD LDFT. We want to point out that in such a geometry the  $H_1$  type of the IUPAC classification is observed. This conclusion is fully justified by the classical concept of the adsorption hysteresis described by Gregg and Sing and the recent DFT and GCMC results. We showed that the strong adsorbate–adsorbent interactions produce multiple steps within hysteresis loops which were observed experimentally. In addition to the other studies of hysteresis

phenomena via the LDFT formalism (see refs 110 and 111), we constructed both ascending and descending scanning curves which are known from experimental observation.<sup>105</sup>

Nowadays, the experimental verification of the obtained computational results is very difficult because, in reality, all materials composed of finite slitlike nanopores (i.e. activated carbons, activated carbon fibers, etc.) are, to more or less an extent, heterogeneous. However, for example, the hysteresis on water adsorption–desorption isotherms measured in small nanopores is a well-known experimental fact.<sup>109</sup> Moreover, this agrees with our modeling, since water adsorption is attributed to the strong specific adsorbate–adsorbent interactions with surface oxides and to strong adsorbate–adsorbate interactions between the clustered molecules forming the hydrogen bonds.

We wish to underline that further experimental as well as theoretical studies of hysteresis in the finite-sized slitlike nanopores will be the subject of our forthcoming correspondence.

**Acknowledgment.** P.K. gratefully acknowledges Professor Aranovich for fruitful correspondence concerning the current paper. The valuable suggestions of the reviewers of this manuscript are also gratefully acknowledged.

**Supporting Information Available:** Figures showing the density profiles and the excess adsorption–desorption isotherms. This material is available free of charge via the Internet at <http://pubs.acs.org>.

LA0501132

(102) Huber, P.; Knorr, K. *Phys. Rev. B* **1999**, *60*, 12657.  
 (103) Naono, H.; Hakuman, M. *J. Colloid Interface Sci.* **1993**, *158*, 19.  
 (104) Gros, S.; Findenegg, G. H. *Ber. Bunsen-Ges. Phys. Chem.* **1997**, *101*, 1726.  
 (105) Machin, W. D. *Langmuir* **1994**, *10*, 1235.  
 (106) Machin, W. D.; Golding, P. D. *J. Chem. Soc., Faraday Trans.* **1990**, *86*, 175.  
 (107) Machin, W. D. *Langmuir* **1999**, *15*, 169.  
 (108) Morishige, K.; Shikimi, M. *J. Chem. Phys.* **1998**, *108*, 7821.  
 (109) Brovshenko, I.; Geiger, A.; Oleinikova, A. *Phys. Chem. Chem. Phys.* **2001**, *3*, 1567.

(110) Libby, B.; Monson, P. A. *Langmuir* **2004**, *20*, 4289.  
 (111) Ravikovitch, P. I.; Neimark, A. V. *Langmuir* **2002**, *18*, 9830.